Canards at Folded Nodes

John Guckenheimer * and Radu Haiduc
Mathematics Department, Ithaca, NY 14853

For Yulij Il'yashenko with admiration and affection on the occasion of his 60th birthday

March 18, 2003

Abstract

Folded singularities occur generically in singularly perturbed systems of differential equations with two slow variables and one fast variable. The folded singularities can be saddles, nodes or foci. Canards are trajectories that flow from the stable sheet of the slow manifold of these systems to the unstable sheet of their slow manifold. Benoît has given a comprehensive description of the flow near a folded saddle, but the phase portraits near folded nodes have been only partially described. This paper examines these phase portraits, presenting a picture of the flows in the case of a model system with a folded node. We prove that the number of canard solutions in these systems is unbounded.

1 Introduction

Folded nodes were apparently discovered by Takens [10] in his study of constrained systems. Benoît [2, 3, 4] pioneered the analysis of *folded singularities* in three dimensional singularly perturbed systems with two slow variables and one fast variable, going beyond Taken's analysis of the singular limit. Following Argemi, he called these *pseudo-singular* points. Smolyan and Wechselberger [9] give a presentation of some of Benoît's results using geometric methods that avoid nonstandard analysis. Mishchenko et al. [8] discuss these problems using classical asymptotic methods and the terminology that folded singularities are jumps that violate the "normal switching conditions." In the case of folded saddles, Benoît's analysis gives a complete description of the local geometry in the neighborhood of the singularity. In the case of a folded node, the local geometry is more intricate and the results are less complete. He establishes in [4] the existence of a pair of *maximal canard* solutions that are distinguished by lying in a specific Gevrey class. In [3], Benoît exhibits examples of canards that do not

*Research partially supported by the Department of Energy and the National Science Foundation.

lie in this class. These more complex canards are associated with oscillations in which a trajectory passing through the region of the folded node makes several turns around one of the distinguished maximal canards, each turn including a jump from the unstable sheet of the slow manifold to the stable sheet of the slow manifold.

This paper develops further insight into the local geometry of flows past folded nodes. Il'yashenko [1] determined a *system of first approximation* for folded singularities whose low order terms depend upon a single parameter a. The derivation of the system of first approximation involves a rescaling of the singular perturbation parameter ε, so the limit system obtained at $\varepsilon = 0$ does not correspond to a uniform approximation of the original problem in a neighborhood of the folded singularity. It represents the behavior of the original problem in an ε-dependent neighborhood of the folded node. We observe that when the parameter a in the system of first approximation is set to zero along with ε, the system has two integrals of motion. When a is negative with small magnitude, we use perturbation methods to give approximations to the more complex canards described above. This is augmented by numerical computations of the systems of first approximation with $\varepsilon = 0$ that identify how the stable and unstable slow manifolds of the system meet at a cross-section passing through the folded node. Using the insight from these computations, we prove that the number of maximal canard trajectories is unbounded as the parameter in the system of first approximation approaches zero. We present numerical calculations that visualize the phase portrait of trajectories passing through the folded node and show the location of the maximal canards.

2 Background

Arnold, Il'yashenko, Rozov, Nejshtadt and Zvonkin [1] reviewed the theory of relaxation oscillations. We describe the setting of this paper using their perspective. A *slow-fast vector field* has the form

$$\begin{aligned} \varepsilon \dot{x} &= f(x, y, \varepsilon) \\ \dot{y} &= g(x, y, \varepsilon) \end{aligned} \tag{1}$$

with $x \in R^m$ and $y \in R^n$. We restrict attention to the case that the fast variable $x \in R$, the slow variables $y \in R^2$. We also assume that the system is generic within the class of smooth slow-fast systems with one fast and two slow variables. The limit $\varepsilon \to 0$ is a *differential algebraic equation*. The solutions of $f = 0$ form a surface, called the *critical manifold* C of the system. In generic slow-fast systems, C is indeed a manifold and at regular points of its projection onto the plane of slow variables ($f_x \neq 0$) the differential algebraic equation can be reduced to an ordinary differential equation, called the *slow flow*, by the implicit function theorem. The regular points of the critical manifold form stable and unstable sheets on which f_x is negative and positive, respectively. The singularities of the projection of C onto the plane of slow variables is the *fold curve* S of the system. In generic systems, except for

isolated *cusps*, the points of S are *fold* singularities [6] of the projection restricted to C. S is a smooth curve at its fold points.

The direction field of the slow flow can be extended to the fold points. As a vector field, this requires a time-rescaling of the slow flow that vanishes on the fold curve and reverses the orientation of trajectories on unstable sheets of the critical manifold. We continue to call this rescaled equation the slow flow of the system. Due to the singularity of the time rescaling, the slow flow of generic systems may have equilibrium points on their fold curves. These equilibrium points are called *folded singularities*, pseudo-singular points [3] or fold points that violate the normal switching conditions [8]. In terms of the system (1), their defining equations are $f = f_x = f_y \cdot g = 0$. Depending on whether the equilibria of the slow flow are saddles, nodes or foci, the folded singularities are called *folded saddles, folded nodes*, *or folded foci*. The folded nodes are the principal topic in this paper.

A local model for folded singularities is given by the system

$$\begin{aligned} \varepsilon\dot{x} &= y - x^2 + \xi \\ \dot{y} &= az + bx + \eta \\ \dot{z} &= 1 + \zeta \end{aligned} \tag{2}$$

with $a \neq 0$, $b \neq 0$ and ξ, η, ζ of higher order. Scaling of the coordinates (x, z, t) by $\sqrt{\varepsilon}$ and y by ε eliminates ε from the left side of the equation for $\dot{x}$ and leaves ξ, η, ζ with order $O(\sqrt{\varepsilon})$. Folded nodes whose slow flows have stable equilibrium points are characterized by $a < 0, b < 0$ and $0 < 1 + 8a/b^2$. Further scaling of the coordinates (x, y) makes $|b| = 1$. Il'yashenko [1] called the result of these scale changes the *system of first approximation* at a folded singularity. He proved that the generic folded singularity can be transformed to the form

$$\begin{aligned} \dot{x} &= y - x^2 + \xi \\ \dot{y} &= az + bx + \eta \\ \dot{z} &= 1 + \zeta \end{aligned} \tag{3}$$

with $|b| = 1$ by smooth ε-dependent coordinate transformations that preserve the foliation by subspaces of fast variables. The limit as $\varepsilon \to 0$ of the system of first approximation can be written as

$$\begin{aligned} \dot{x} &= y - x^2 \\ \dot{y} &= az \pm x \\ \dot{z} &= 1 \end{aligned} \tag{4}$$

A stable folded node occurs when the sign of x in the second equation is negative, $a < 0$ and $1 + 8a > 0$. *We henceforth restrict ourselves to this case without explicitly restating these properties of* (4).

3 The System of First Approximation: Geometry

We study phase portraits of the systems (4) and (2) in the remainder of this paper. Properties of (4) that are structurally stable will be valid for the system (3) when $\varepsilon > 0$ is sufficiently small. Well established theory for slow-fast systems proves that trajectories of (2) that are not close to the fold curve along the z-axis will either tend to an ε-neighborhood of the critical manifold or to infinity on the fast time scale. Truncating the equations (2) by dropping the terms ξ, η, ζ, setting $\varepsilon = 0$, rescaling time and using (x, z) as coordinates on the critical manifold, motion along the critical manifold is approximated by trajectories of the slow flow equations

$$\begin{aligned} \dot{x} &= az + bx \\ \dot{z} &= 2x \end{aligned} \tag{5}$$

This is a linear system whose solution is elementary. With $b = -1$, there are two negative eigenvalues $-1/2 \pm \sqrt{1 + 8a}/2$ and their eigendirections both have negative slope. The weak stable direction is along the eigenvector that is closer to the z-axis. Note that trajectories in the (x, z) plane with initial conditions between the fast eigenvector and the negative z-axis approach the origin tangent to the weak eigenvector, while trajectories between the fast eigenvector and the positive x-axis cross the x-axis before reaching the z-axis. Trajectories with initial conditions on $x = 0, z < 0$ advance into the half plane $x > 0$ and approach the origin along the weak eigendirection.

Maximal canards of (2) are defined to be trajectories that remain on the slow manifold for all time. Since the coordinate z increases at unit rate in the three dimensional flow of (2) and the solutions of (5) are defined for all time, the maximal canards will cross every plane $z = c$, c constant, close to the critical manifold. We develop a strategy to compute the maximal canards by locating the intersections of the stable and unstable sheets of the slow manifold with $z = 0$. Initial conditions in the plane $z = -c$ will approach the slow manifold on the fast time scale and follow it, staying close to a trajectory of the slow flow until they reach the vicinity of the fold curve. This is embodied in the existence of a *strong stable foliation* of the slow manifold [5]. Each trajectory with initial conditions in the critical manifold and $z = -c$ lies in a leaf of the strong stable foliation of the slow manifold. Since the slow flow crosses the negative z-axis pointing away from the fold, the only places that the trajectories starting at $z = -c$ can approach the fold curve are near the origin or with $z > 0$. Roughly speaking, the trajectories that lie between the fast eigendirection and the negative z-axis approach the origin, while the trajectories between the fast eigenvector and the positive x-axis will reach the positive z-axis. The trajectories that reach $x = 0$ with $z > 0$ flow to infinity in finite time along curves that are almost parallel to the negative x-axis.

To find the maximal canards, we use numerical integration to follow trajectories of the system (4) with initial conditions on the curve that is the intersection of the critical manifold $y = x^2$ with a plane $z = -c$. We compute the intersections of these trajectories with the plane $z = 0$. If c is sufficiently large, the trajectories approach the slow manifold and follow it to its intersection with $z = 0$. Since the trajectories follow the stable sheet of the

slow manifold, their endpoints give an approximation to Z_s, the intersection of the stable slow manifold with $z = 0$. Note that the system (4) has the time reversing symmetry $\sigma(x, y, z, t) = (-x, y, -z, -t)$. The plane $z = 0$ is invariant under the symmetry σ, so $Z_u = \sigma(Z_s)$ will be the intersection of the unstable slow manifold with $z = 0$. The points of intersection of Z_s and Z_u lie on maximal canards since they arrive on trajectories lying in the slow manifold and their forward trajectories lie on the unstable sheet of the slow manifold. Figure 1 gives this approximation to Z_s and $Z_u = \sigma(Z_s)$, computed with $c = -200$ and $a = -0.002$. Figure 2 shows a blow-up of the spirals near their cores. There appear to be approximately 50 transverse intersections of Z_s and Z_u, all on the y-axis. The spirals in the figure suggest a readily discernible pattern to the structure of Z_s and Z_u. We use perturbation methods in the next section to explore these patterns in the limit that a approaches 0.

4 Perturbation analysis

The sign of a in system (4) determines whether there is a folded node or saddle. At the transition $a = 0$, the system separates, with the motion in the (x, y) directions independent of z. Moreover, the (x, y) motion of the system is reversible (has a time-reversing reflectional symmetry) and has the first integral

$$H(x, y) = \exp(-2y)(y - x^2 + \frac{1}{2})$$

The level curve $H = 0$ is the parabola $y - x^2 + 1/2 = 0$. Level curves above $H = 0$ are closed curves in the (x, y) plane. The level curves with $H < 0$ are unbounded and the corresponding trajectories tend to infinity in finite time, asymptotically parallel to the x-axis. The origin is a center for the (x, y) subsystem.

For $a < 0$ of small magnitude, we can use the variation of H along trajectories to help compute their motion. As long as the trajectories remain in the region where $H > 0$, we expect their projections into the (x, y) plane to make loops around the origin. When they pass into the region where $H < 0$, they can be expected to tend to infinity in finite time. Consider the simpler problem

$$\begin{aligned} \dot{x} &= y - x^2 \\ \dot{y} &= \beta - x \end{aligned} \tag{6}$$

with β fixed at a representative value of az in the region of interest. The system (6) rescaled by the "integrating factor" $\exp(-2y)$ to

$$\begin{aligned} \dot{x} &= \exp(-2y)(y - x^2) \\ \dot{y} &= \exp(-2y)(\beta - x) \end{aligned} \tag{7}$$

has divergence

$$-2\beta \exp(-2y)$$

Clearly, this divergence vanishes when $\beta = 0$, so the Bendixson criterion [7] can be applied to (7). This criterion determines how the closed trajectories of (7) vary with β when $\beta \neq 0$ has small magnitude. In particular, the distance of a Poincaré map from the identity of (7) is approximated by the integral of the divergence of (7) over the interior of closed trajectories of the system with $\beta = 0$. Since the divergence has opposite sign to β, all trajectories of (7) spiral toward or away from the origin. When $\beta > 0$, trajectories spiral toward the equilibrium; when $\beta < 0$, trajectories spiral away from the equilibrium. Note also that the divergence is an exponentially decreasing function of y. Since the level curves of H with $H > 0$ large are approximated by segments of the parabola $y - x^2 + 1/2 = 0$ with a horizontal segment along $y = y_c$, the magnitude of the divergence integral grows slowly with y_c when y_c is large.

This analysis suggests that in the regime that $a < 0$ has small magnitude and $az > 0$ is small, trajectories of (4) spiral toward the z-axis. When z changes sign, the trajectories begin to spiral away from the z-axis. This picture is only suggestive, however, because z increases along solutions of (4). Benoît observed that there are precisely two trajectories of (4) that are algebraic. These are given by

$$(x, y, z) = (\alpha t, \alpha + \alpha^2 t^2, t)$$

where $2\alpha^2 + \alpha - a = 0$. Note that when the magnitude of $a < 0$ is small, the values of α are approximately $-1/2$ and a. Introducing coordinates along an algebraic trajectory

$$\begin{aligned} \xi &= x - \alpha t \\ \eta &= y - \alpha - \alpha^2 t^2 \\ \zeta &= z - t \end{aligned} \tag{8}$$

the system (4) is transformed to

$$\begin{aligned} \dot{\xi} &= -2\alpha t \xi + \eta - \xi^2 \\ \dot{\eta} &= -\xi \\ \dot{\zeta} &= 0 \end{aligned} \tag{9}$$

When t is small the linear part of this system has complex eigenvalues, which suggests switching to polar coordinates in the (ξ, η) plane. With $(\xi, \eta) = (r\cos(\theta), r\sin(\theta))$, the system (9) becomes

$$\begin{aligned} \dot{r} &= -2\alpha t r \cos^2(\theta) + r^2 \cos^3\theta \\ \dot{\theta} &= -1 + \alpha t \sin(2\theta) + r\cos^2(\theta)\sin(\theta) \\ \dot{t} &= 1 \end{aligned} \tag{10}$$

The cylinder $\{r = 0, \theta, t\}$ is invariant for the system (10), being a blown up image of the canard trajectory we started from. We are interested in how trajectories of (10) move on this surface, as this shows us how trajectories of (4) wind around the algebraic trajectories. Setting $r = 0$ in (10) gives

$$\dot{\theta} = -1 - \alpha t \sin(2\theta) \tag{11}$$

When t is positive but less than $t^* = -1/\alpha$, θ is strictly increasing. At time $t = t^*$ we have $\dot{\theta} > 0$ everywhere except at the points $\theta_1 = -\pi/4$ and $\theta_2 = 3\pi/4$. As we increase t beyond t^*, each θ_j splits into two points θ_{j1} and θ_{j2}, giving us four zeros of $\dot{\theta}$ at each time t. As $t \to \infty$ the points $\theta_{11} \to -3\pi/4$, $\theta_{12} \to 0$, $\theta_{21} \to \pi/2$ and $\theta_{22} \to \pi$. The set of zeros of $\dot{\theta}$ on the infinite cylinder $\{r = 0, \theta, t > 0\}$ will consist of four curves connecting the points $\theta_j(t^*)$ and $\theta_{jk}(\infty)$. Since $\theta_{jk}(t) \neq 0$ for t^*, t, these curves do not rotate, and the solutions of (11) do not make a complete rotation when $t > t^*$. Thus, the only rotations occur when $t < t^*$. To estimate how many rotations a solution makes, we observe that equation (11) with $0 < t < t^*$ implies

$$-1 + \alpha t < \dot{\theta} < -1 - \alpha t$$

Integrating this we get

$$\alpha(t^*) - \alpha(0) \in (\frac{3}{2\alpha}, \frac{1}{2\alpha})$$

Therefore, the number of complete rotations is of order $O(|1/\alpha|)$. The same analysis applies for negative t, so we can conclude that when $|t|$ is small enough, the flow rotates around the algebraic trajectory with $\alpha \approx a$. This rotation takes place for a finite period of time, and the total number of rotations of nearby trajectories is of order $O(|1/\alpha|)$.

We next argue that initial conditions for the system (4) that start on the y-axis with $y > 0$ large do not complete a full rotation around the z-axis. This is more readily seen by transforming to coordinates with y being replaced by $u = y - x^2 + 1/2$. In these coordinates, (4) becomes

$$\begin{aligned} \dot{u} &= az - 2ux \\ \dot{x} &= u - 1/2 \\ \dot{z} &= 1 \end{aligned} \tag{12}$$

and the algebraic trajectories move uniformly along lines: $(u, x, z) = (\alpha + 1/2, \alpha t, t)$. When $az < 0$ and $ux \geq 0$, $\dot{u} < 0$ and $\dot{x} < 0$. Thus, the region with $u < 0, x < 0$ and $z > 0$ is invariant. We follow a trajectory with initial condition $(u_0, 0, 0)$ on the u-axis with $u_0 > 0$ large. While u remains large, the trajectory stays close to the parabolic surface $u + x^2 = u_0$. As long as $u > 1/2$, x continues to increase and u decreases. Thus we reach a point on the surface $u = 1/2$ at $(1/2, x_1, z_1)$ with the magnitude of x_1 comparable to $\sqrt{u_0}$. As $u_0 \to \infty$, $x_1 \to \infty$. In the region $0 < u < 1/2, x > 0, z > 0$, $1/2 > \dot{x} > 0$ and $\dot{u} < az = at$. Therefore, $1/2 - u(t) > a(t_1^2 - t^2)/2 > at^2/2$. Thus, by time $t = \sqrt{-1/a}$, the trajectory must reach either $u = 0$ or $x = 0$. If $2x_1 > \sqrt{-1/a}$, the trajectory reaches $u = 0$ with x still positive. Since $\dot{u} < 0$ when $u = 0$ and $z > 0$, the trajectory never returns to $u = 0$. In particular, the trajectory never completes a loop around the z-axis.

The unstable sheet of the slow manifold of system (4) separates trajectories that tend to ∞ with x decreasing from trajectories that cross the plane $x = 0$ with x increasing. Between any two points on the y-axis whose trajectories make a different number of turns around the z-axis for $t > 0$, there must be a point whose trajectory remains close to the slow manifold as $t \to \infty$. We have demonstrated that the number of turns varies from 0 to a number

that is $O(-1/a)$. Therefore, the set of points on the y-axis whose trajectories flow along the unstable sheet of the slow manifold for all time has cardinality $O(-1/a)$. Using the symmetry of system (4), the same points have backward trajectories that flow on the stable sheet of the slow manifold for all time. Summarizing this discussion, we have proved the following.

Theorem: As $a \nearrow 0^-$, the truncated system of first approximation for a folded node, system (4), has an unbounded number of trajectories that remain at a bounded distance from its critical manifold for all time. There are $O(-1/a)$ such trajectories that intersect the y-axis.

5 More Geometry and Conjectures

We would like to extend our perturbation analysis to give a more complete picture of the trajectories of system (4) flowing through the region of a folded node. The plane $z = 0$ is a cross-section to the flow that is mapped into itself by the time reversing symmetry σ. We expect that points starting in this plane either track the unstable sheet of the slow manifold or tend to infinity in finite time along trajectories that are asymptotically parallel to the x-axis. Figures 3 and 4 visualize the fate of trajectories with initial conditions in the plane $z = 0$ for system (4) with a = -0.002. A grid of 500×500 points was selected in the rectangle $[-1.25, 1.25] \times [-0.5, 2]$ and followed to the intersection of these trajectories with the plane $x = -50$. This value of x has large enough magnitude that x will continue to decrease monotonically on all these trajectories after they pass through $x = -50$. Figure 3 displays a pseudocolor plot of the y coordinates of the final points of the trajectory segments as a function of the (x, y) coordinates of their initial points. There is an apparent discontinuity in the value of the y coordinate along a spiral that looks like the intersection of the unstable unstable sheet of the slow manifold with $z = 0$ displayed in Figure 1. These are indeed points that flow along the unstable sheet of the slow manifold for a long time. Points on the convex side of the discontinuity leave the unstable sheet with x decreasing monotonically toward ∞. Points on the concave side of the discontinuity make an additional turn around the algebraic canard after they leave the unstable sheet for the last time, then head toward ∞ with a small value of y. Figure 4 displays a pseudocolor plot of the z coordinate of the final points of the trajectory segments as a function of the (x, y) coordinates of their initial points. Darker points have terminal points with larger values of z, and hence take longer to reach the plane $x = -50$. Here the extra time associated with flowing along the unstable sheet of the slow manifold is not resolved near the discontinuities of the spiral. Instead, one sees the contribution to the time length of the trajectory from making an additional turn around the algebraic canard. The "tongues" that are visible in the picture illustrate that the points closer to the unstable slow manifold take longer to reach ∞ than the points that are farther away. Figures 3 and 4 together give a relatively complete picture of how trajectories with initial conditions evolve in forward time. The corresponding picture for the evolution of trajectories in backward time is obtained by reflecting these pictures in the y-axis. Based upon these pictures, we make the following conjecture.

Conjecture: Assume that $a < 0$ has small magnitude. All solutions of system (4) that are defined for all time lie on the intersection of the stable and unstable sheets of the slow manifold and are symmetric with respect to the symmetry σ. With possibly the exception of the algebraic solution that intersects the y-axis near $y = a$, all of the intersections of the stable and unstable sheets of the slow manifold in the plane $z = 0$ are transverse.

This note analyzes system (4). However, since the distinguished canards persist when higher order terms are restored to the system of first approximation [4], we believe that the dynamics we have described apply to all systems with folded nodes.

References

[1] Arnold, V. I., Afrajmovich, V. S. Il'yashenko, Yu. S. and Shil'nikov, L.P. *Dynamical Systems V.* Encyclopaedia of Mathematical Sciences. Springer-Verlag, 1994.

[2] Benoît, É. Systmes lents-rapides dans R^3 et leurs canards. Third Schnepfenried geometry conference, Vol. 2 (Schnepfenried, 1982), 159–191, Astrisque, 109-110, Soc. Math. France, Paris, 1983.

[3] Benoît, É. Canards et enlacements *Publ. Math. IHES Publ. Math.* **72**(1990) 63–91

[4] Benoît, É. Perturbation singulire en dimension trois: canards en un point pseudo-singulier nœud. Bull. Soc. Math. France 129 (2001), no. 1, 91–113.

[5] Fenichel, N. Geometric singular perturbation theory. *J. Diff. Eq.*, 31 (1979), 53–98, 1979.

[6] Golubitsky, M. and Guillemin, V. Stable mappings and their singularities, Springer-Verlag, 1973.

[7] Guckenheimer, J. and Holmes, P. *Nonlinear Oscillations, Dynamical Systems, and Bifurcations of Vector Fields*. Springer-Verlag, New York, 1983.

[8] Mishchenko, E. Kolesov, Yu. Kolesov, A. and Rozov, N. *Asymptotic methods in singularly perturbed systems* (Translated from the Russian by Irene Aleksanova. New York: Consultants Bureau), 1994.

[9] Szmolyan, P. and Wechselberger, M. Canards in R^3 *J. Diff. Eq.*, **177** (2001) 419–453

[10] Takens, F. Constrained equations; a study of implicit differential equations and their discontinuous solutions, in: Structural stability, the theory of catastrophes, and applications in the sciences, LNM **525**, Springer-Verlag, 1976.

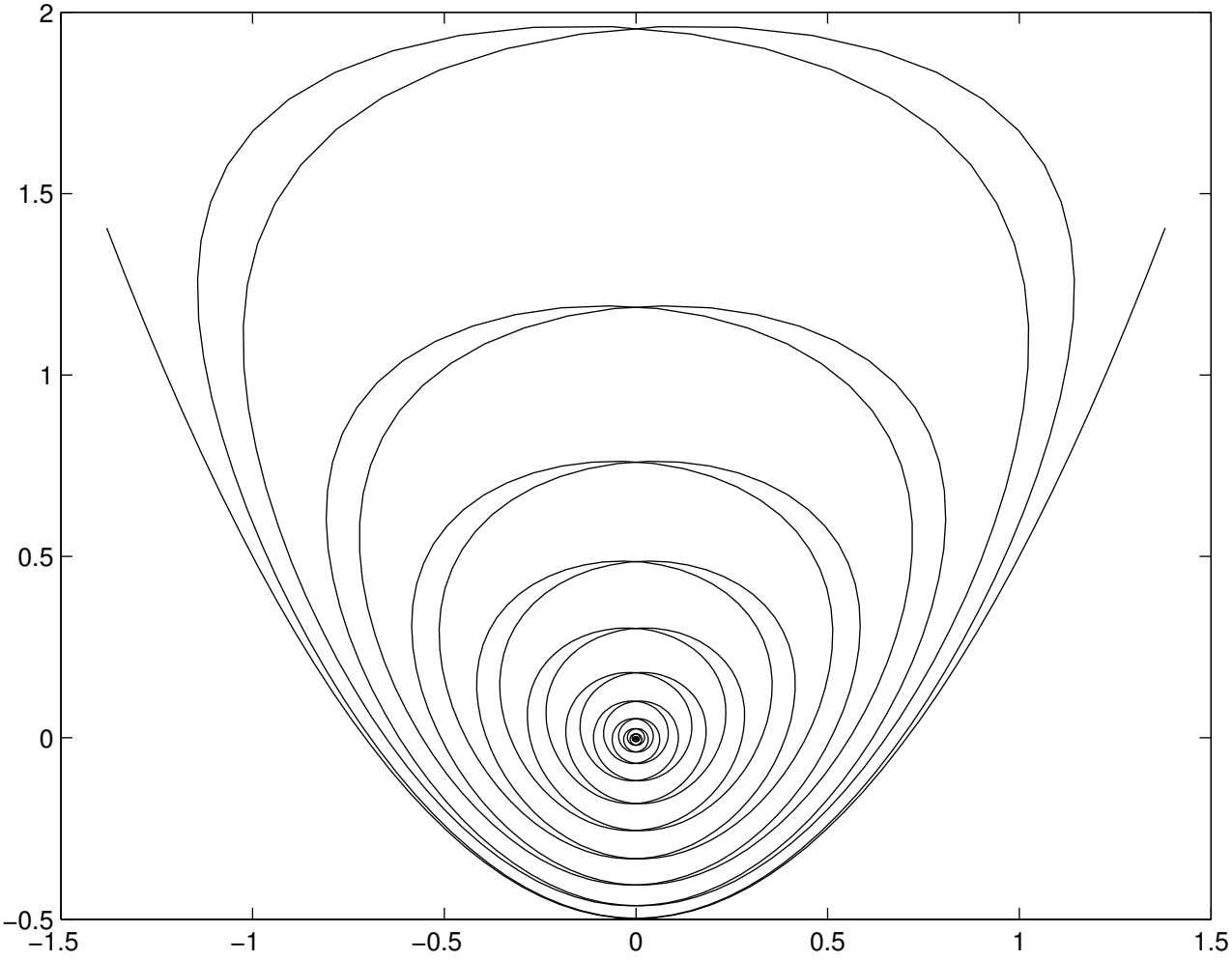

Figure 1: Z_s and Z_u, the intersections of the stable and unstable sheets of the slow manifold of the system (4) with the plane $z = 0$. The parameter $a = -0.002$. To obtain Z_s, trajectories with initial conditions along the curve $(x, x^2, -50), 0 < x < 25$ were computed until $t = 50$. The unstable sheet was obtained by applying the symmetry σ to Z_s.

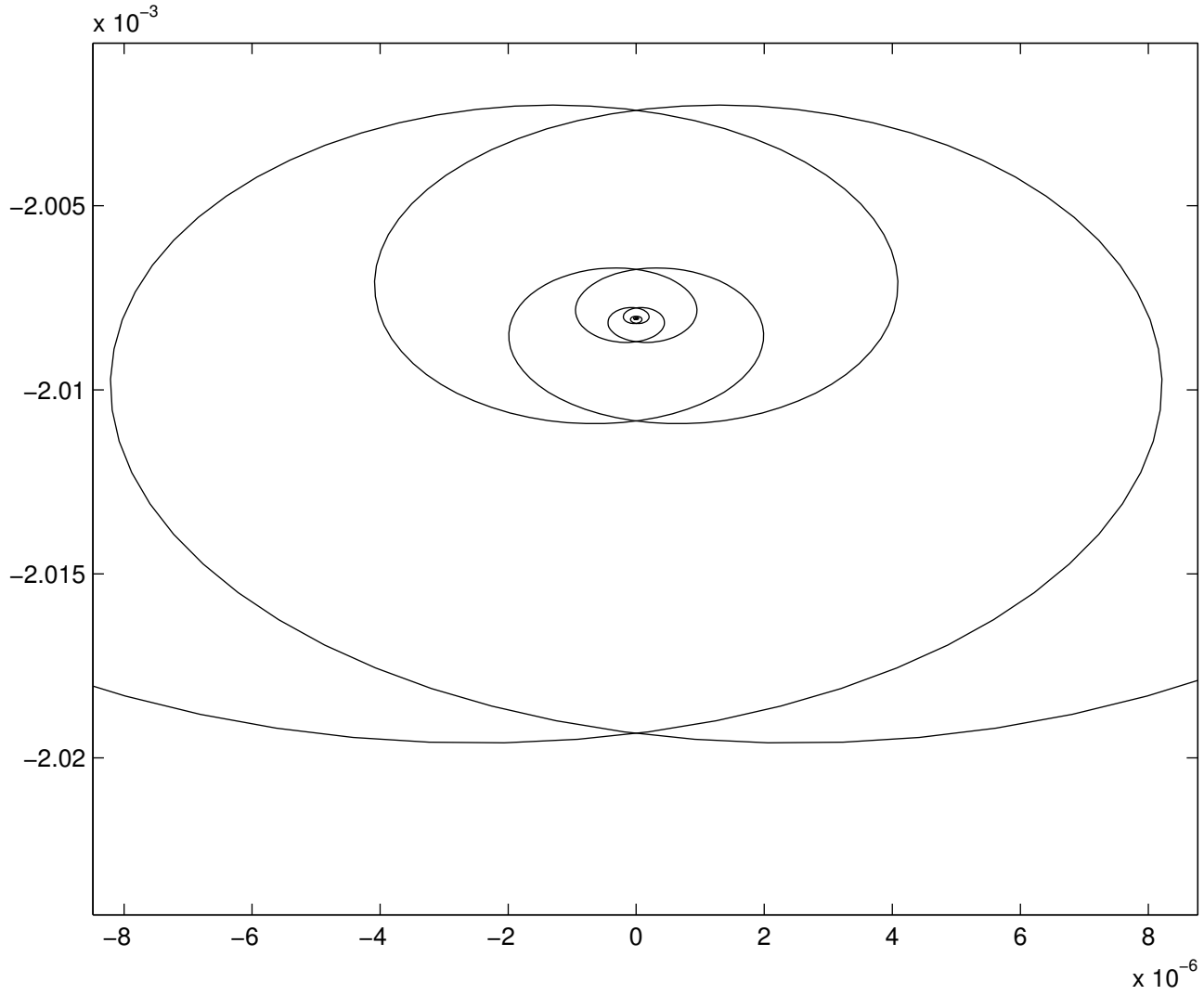

Figure 2: A small portion of the spirals in Figure 1 near their cores.

Figure 3: Trajectories starting on the plane $z = 0$ are computed until they intersect the plane $x = -50$. The color intensity of each point in the figure is determined by the y coordinate of the endpoint of the trajectory segment. Darker colors correspond to larger values of y.

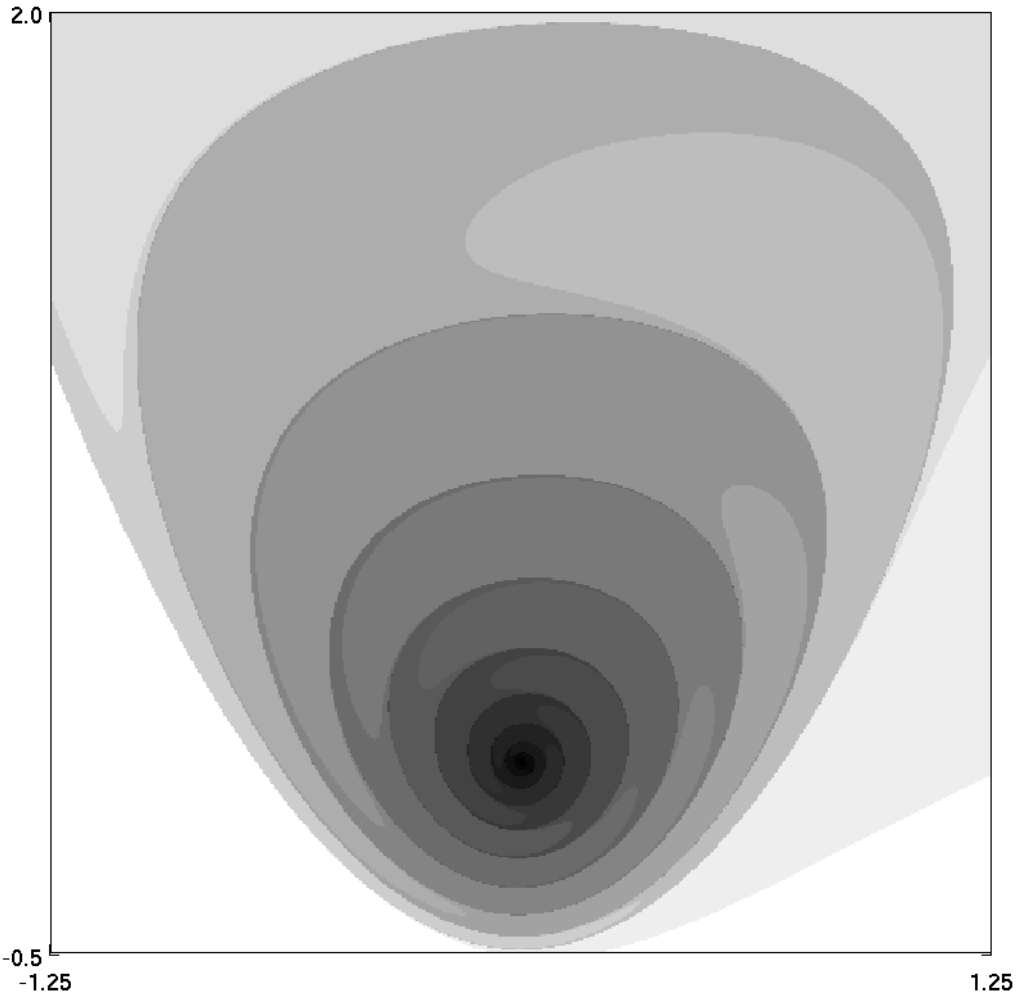

Figure 4: Trajectories starting on the plane $z = 0$ are computed until they intersect the plane $x = -50$. The color intensity of each point in the figure is determined by the z coordinate of the endpoint of the trajectory segment. Darker colors correspond to larger values of z.